

RSC Advances



This is an *Accepted Manuscript*, which has been through the Royal Society of Chemistry peer review process and has been accepted for publication.

Accepted Manuscripts are published online shortly after acceptance, before technical editing, formatting and proof reading. Using this free service, authors can make their results available to the community, in citable form, before we publish the edited article. This *Accepted Manuscript* will be replaced by the edited, formatted and paginated article as soon as this is available.

You can find more information about *Accepted Manuscripts* in the [Information for Authors](#).

Please note that technical editing may introduce minor changes to the text and/or graphics, which may alter content. The journal's standard [Terms & Conditions](#) and the [Ethical guidelines](#) still apply. In no event shall the Royal Society of Chemistry be held responsible for any errors or omissions in this *Accepted Manuscript* or any consequences arising from the use of any information it contains.

Microwave directed metal-free regiodivergent synthesis of 1,2-teraryls and study of supramolecular interactions

Received 00th January 20xx,
Accepted 00th January 20xx

DOI: 10.1039/x0xx00000x

www.rsc.org/

Surjeet Singh,^{a,†} Shally,^{a,†} Ranjay Shaw,^{a,†} Reena Yadav,^b Abhinav Kumar^b and Ramendra Pratap^{a,*,†}

A Microwave directed, simple and efficient synthesis of 2-amino-3,4-diaryl-6-(sec.amino)-benzonitrile has been delineated through ring transformation reaction of 6-aryl-2-oxo-4-sec-amino-2H-pyran-3-carbonitriles by benzyl cyanide under basic conditions. Reaction of 6-aryl-4-sec-amino-2-oxo-2H-pyran-3-carbonitriles and benzyl cyanide in DMSO and KOH as a base at 15°C provides (2E,4E)-5-aryl-6-oxo-6-phenyl-3-sec-amino-hexa-2,4-dienitriles. Reaction of 6-phenyl-4-(piperidin-1-yl)-2-oxo-2H-pyran-3-carbonitrile and benzyl cyanide in DMF and sodamide at 100 °C provides 1,5-diphenyl-3-(piperidin-1-yl)cyclopenta-2,4-diene-1,2-dicarbonitrile. Use of Microwave irradiation divert the regioselectivity and change the course of reaction and 1,2-teraryls was isolated. Structure of one of the compound was confirmed by single crystal X-ray and the nature of weak interactions in the compound has been addressed using *ab initio*, Atoms in Molecules (AIM) and Hirshfeld surface analysis.

Introduction

Regiodivergent synthetic approach is an interesting concept and various research groups are now focused to explore these possibilities.¹ Change of any component of reaction as catalyst, temperature, duration of reaction, stoichiometry of precursors and atmospheric condition can completely divert the path of reaction and different product can be obtained regioselectively.¹ It is always important to explore the diverse reactivity of any precursor under various condition and so we are encouraged to explore our precursor for the same.

1,2-diarylbenzenes are reported as an important class of compounds, resulting from aromatic system as exceptional building block.² These highly functionalized teraryls exhibit wide applications as laser dyes,² liquid crystals³ and conducting polymers.⁴ Functionalized 1,2-teraryl skeleton is also present in various natural products⁵ and medicinally important compounds as subunit and enhance their therapeutic potential.⁶ Presence of amino group in teraryls make them a strategically important precursor for synthesis of agrochemicals, dyes, pharmaceuticals, pigments and polymers.⁷ This type of aminated teraryls are also useful for the synthesis of biologically and pharmaceutically important compound like carbazoles,⁸ estrogen receptors,⁹ anti-HIV agent Siamenol,¹⁰ antihyperglycemic agents¹¹ and synthesis of diimine Ni(II) and Pd(II) complexes used for the polymerization of ethylene and methyl acrylate.¹²

Recently, various approaches for the synthesis of

functionalized teraryls have been used such as; Palladium-Catalyzed annulation strategy of alkynes and (2-iodophenyl)acetonitrile,¹³ metal-free arylation of anilines,¹⁴ Pd-Catalyzed Semmler–Wolff reactions¹⁵ and Diels–Alder cycloadditions reactions¹⁶ The previous reports indicated that presence of amino group in precursor hinder the C–C bond formation reactions. A wide range of catalytic systems have been established for synthesis of satirically hindered teraryls and require harsh reaction conditions, expensive metal catalysts and ligands (Figure 1).

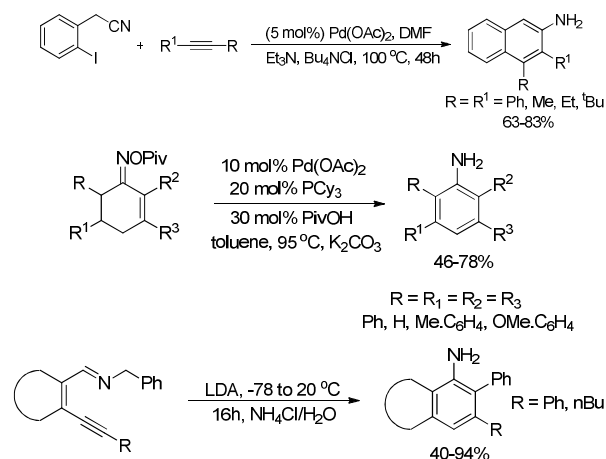


Fig. 1. Present methodologies for the synthesis of aminated teraryl skeleton

^a Department of Chemistry, University of Delhi, North campus, Delhi, India-110007; Tel: +911127666646; E-mail: ramendrapratap@gmail.com

^b Department of Chemistry, University of Lucknow, Lucknow, Uttar Pradesh, India-226009.

^c Address here.

[†] SS, RS and RP were involved in methodology development and AK worked on X-ray crystallographic and computational study.

Electronic Supplementary Information (ESI) available: 1H and 13C NMR data of all the synthesized compounds are provided in SI. See DOI: 10.1039/x0xx00000x

Result and Discussion

Herein, we wish to report regiodivergent, metal-free, simple, economical and base mediated Microwave assisted synthesis of 2-amino-6-aryl-4'-substituted-4-sec-amino-1-[1,1'-biphenyl]-3-carbonitriles by reaction of 6-aryl-2-oxo-4-sec-amino-2H-

Method

Organic Chemistry Frontiers

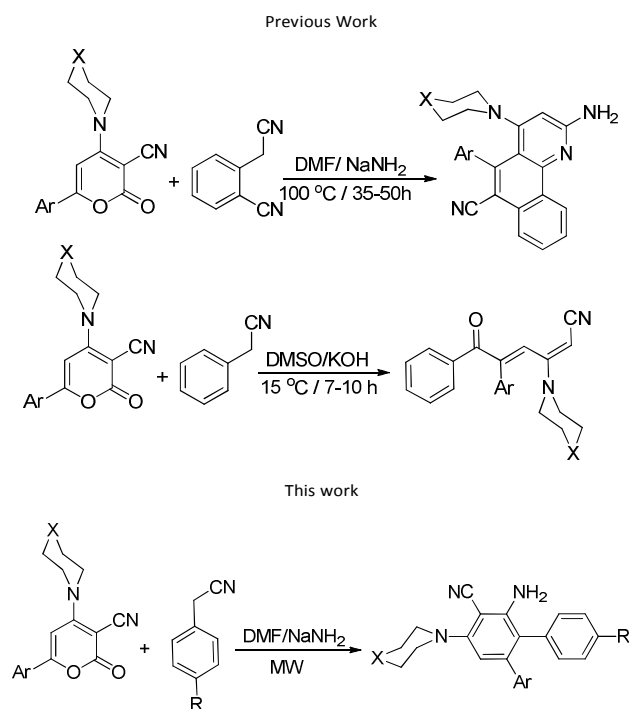
pyran-3-carbonitriles using benzyl cyanide as a carbanion source.

Recently, we have observed that reaction of 6-aryl-2-oxo-4-sec.amino-2H-pyran-3-carbonitriles and 2-cyanomethylbenzonitrile presence of base at 100 °C provided arylated 2-aminobenzo[h]quinolines.¹⁷ In another reaction, stirring of 6-aryl-2-oxo-4-sec.amino-2H-pyran-3-carbonitriles and benzyl cyanide under basic conditions at 15°C provides (2*E*,4*E*)-5-aryl-6-oxo-6-phenyl-3-sec.amino-hexa-2,4-

In order to perform the synthesis of 2-amino-6-aryl-4'-substituted-4-sec.amino-1-[1,1'-biphenyl]-3-carbonitriles **6**, 6-aryl-2-oxo-4-sec.amino-2H-pyran-3-carbonitriles **4** has been selected as precursor. 6-Aryl-4-sec.amino-2-oxo-2H-pyran-3-carbonitriles **4** was synthesized in two steps.

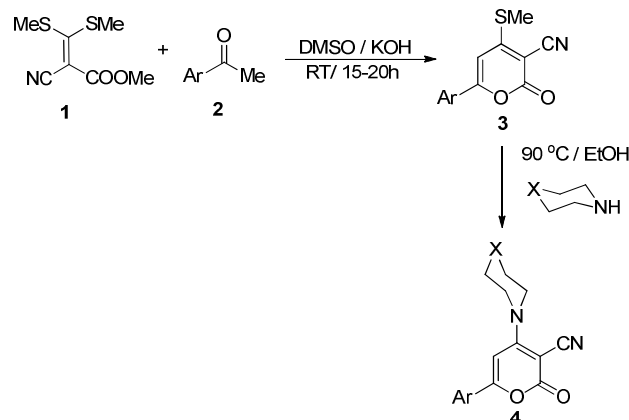
6-Aryl-4-methylthio-2-oxo-2H-pyran-3-carbonitriles **3** was synthesized by stirring an equimolar mixture of 2-cyano-3,3-bis-methylsulfanyl-acrylate **1** and functionalized acetophenones in DMSO in presence of base. Presence of SME group at C4 position makes it highly electrophilic in nature, and undergoes some side reactions during ring transformation approach. To reduce the electrophilicity of position C-4, 6-aryl-2-oxo-4-sec.amino-2H-pyran-3-carbonitriles **4** was synthesized by reaction of **3** and various secondary amines in refluxing ethanol (Scheme 2).¹⁹

Recently, it was observed that reaction of 6-aryl-4-sec.amino-2-oxo-2H-pyran-3-carbonitriles **4** and benzyl cyanide provides highly functionalized enones. We have also observed that under nitrogen atmosphere no ketone formation occur and carbanion generated from benzyl cyanide attack at C-6 position of pyran followed by decarboxylation to afforded dinitrile compound.



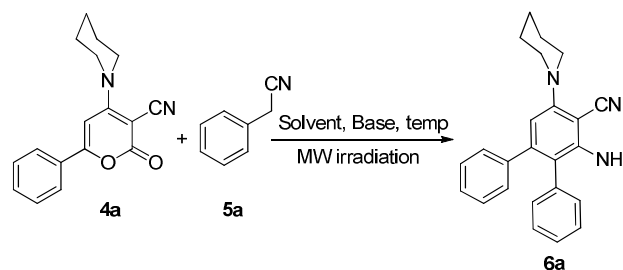
Scheme 1. Previous work versus this work

dienitriles through decarboxylation and oxidative decyanation in presence of aerial atmosphere.¹⁸ Here, we have studied the reaction of 6-aryl-2-oxo-4-sec.amino-2H-pyran-3-carbonitrile and benzyl cyanide under Microwave irradiation conditions.



Scheme 2. Synthesis of 6-aryl-4-sec.amino-2-oxo-2H-pyran-3-carbonitriles **4**

Table 1. Optimization of reaction condition



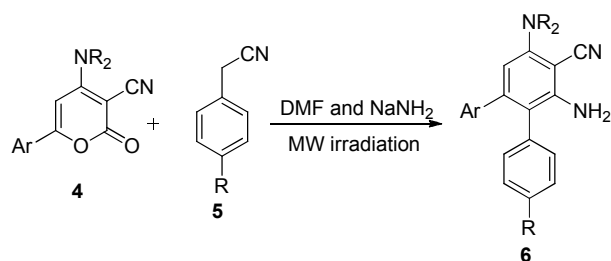
Entry	Base	Solvent	Temp (°C)	Time (minute)	6a (%)
1	KOH	DMSO	80	10	Reaction incomplete
2	KOH	DMSO	80	15	Reaction incomplete
3	KOH	DMSO	80	20	Reaction incomplete
4	KOH	DMSO	100	20	30
5	KOH	DMF	100	20	33
6	NaH	DMF	100	20	30
7	NaNH ₂	DMF	100	20	70
8	NaNH ₂	DMSO	100	20	25
9	NaNH ₂	DMF	120	20	35

All reactions were performed under Microwave irradiation using 2-oxo-6-phenyl-4-piperidin-1-yl-2H-pyran-3-carbonitrile **4a** (0.5 mmol) and benzyl cyanide **5a** (0.5 mmol) in various solvent (2.0 mL) and base (0.75 mmol) at different temperature.

Recently, we have reported that stirring of mixture of 2-oxo-4-piperidin-1-yl-6-thiophen-2-yl-2H-pyran-3-carbonitrile and phenyl-acetonitrile in DMSO in presence of KOH at room temperature under nitrogen atmosphere provided mixture of two isomeric compounds characterized as (2*E*,5*Z*)-2-phenyl-5-(piperidin-1-yl)-3-(thiophen-2-yl)hepta-2,5-dienedinitrile and (2*E*,4*E*)-2-phenyl-5-(piperidin-1-yl)-3-(thiophen-2-yl)hepta-2,4-

dienedinitrile.¹⁸ This result enhanced our interest and we started to look for some reaction conditions, which can give ring transformation to afford 1,2-teraryls. For screening of reaction conditions, we have chosen 2-oxo-6-phenyl-4-piperidin-1-yl-2H-pyran-3-carbonitrile **4a** and benzyl cyanide as model substrates. We have started our screening using KOH and DMSO and irradiated the reaction mixture at 80 °C for 10 minute under Microwave. Reaction was monitored by TLC, which shows the presence of desired compound and left starting material (table 1, entry 1). Further, we have tried the similar reaction condition for 15 and 20 minutes and same result were obtained (table 1, entry 2 and 3). Then, we have used the same combination and irradiated at 100 °C for 20 minute under microwave condition. At higher temperature reaction was completed with formation of 30% of the desired product (table 1, entry 4). In another trial, DMSO was replaced with DMF and to get desired product in 33% yield (table 1, entry 5). Then we have optimized reaction in DMF and DMSO using sodium hydride and sodium amide as a base at different temperature under microwave irradiation (table 1, entry 6-9). From optimization result, we have established the best reaction condition for the synthesis of 2-amino-6-aryl-4'-substituted-4-sec.amino-1-[1,1'-biphenyl]-3-carbonitrile **6a** (table 1, entry 7). So heating of reactants in DMF in presence of sodamide at 100 °C for 20 minutes under microwave irradiation afford the desired product.

Scheme 3 Synthesis of functionalize 2-amino-6-aryl-4'-substituted-4-sec amino-1-yl-[1,1'-biphenyl]-3-carbonitrile.



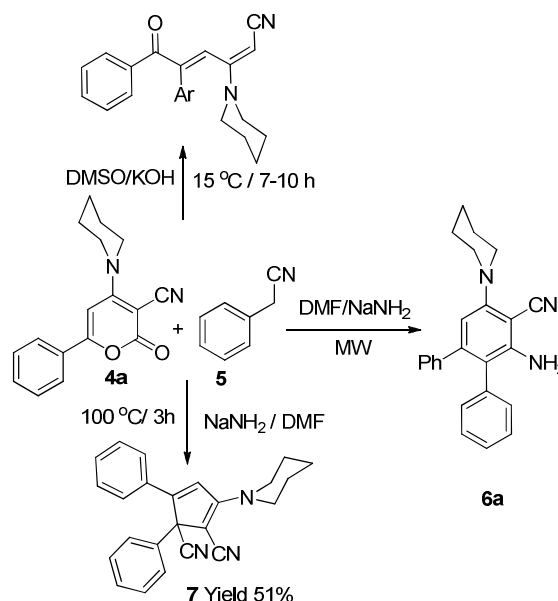
6	Ar	NR ₂ '	R	Yield (%)
6a	C ₆ H ₅	Piperidin-1-yl	H	70
6b	<i>p</i> -CH ₃ .C ₆ H ₄	Piperidin-1-yl	H	64
6c	<i>p</i> -Cl.C ₆ H ₄	Piperidin-1-yl	H	59
6d	<i>p</i> -Cl.C ₆ H ₄	Piperidin-1-yl	OMe	58
6e	<i>p</i> -F.C ₆ H ₄	Piperidin-1-yl	H	58
6f	Thienyl	Piperidin-1-yl	H	62
6g	C ₆ H ₅	4-Morpholin-1-yl	H	65
6h	<i>p</i> -Br.C ₆ H ₄	4-Morpholin-1-yl	OMe	62
6i	<i>p</i> -Cl.C ₆ H ₄	4-Morpholin-1-yl	H	64
6j	<i>p</i> -F.C ₆ H ₄	4-Morpholin-1-yl	OMe	64

All reaction performed under Microwave irradiation with 6-aryl-2-oxo-4-sec-amino-1-yl-2H-pyran-3-carbonitrile (0.5 mmol) and substituted phenylacetonitrile (0.5 mmol) in DMF (2mL) and presence of NaNH₂ (0.75 mmol) 1.5eq at 100 °C for 20 minute.

Generality of the reaction condition was tested for the synthesis of various functionalized teraryls, 2-amino-6-aryl-4'-substituted-4-sec.amino-1-[1,1'-biphenyl]-3-carbonitriles (Scheme 3) **6a-j**. We have observed that presence of electron

donating and withdrawing group in aryl ring at position 6 of pyran do not play any major role in the variation of yields of the products.

Scheme 4. Comparison of various reaction conditions on the reaction of 2H-pyran-2-one and benzyl cyanide

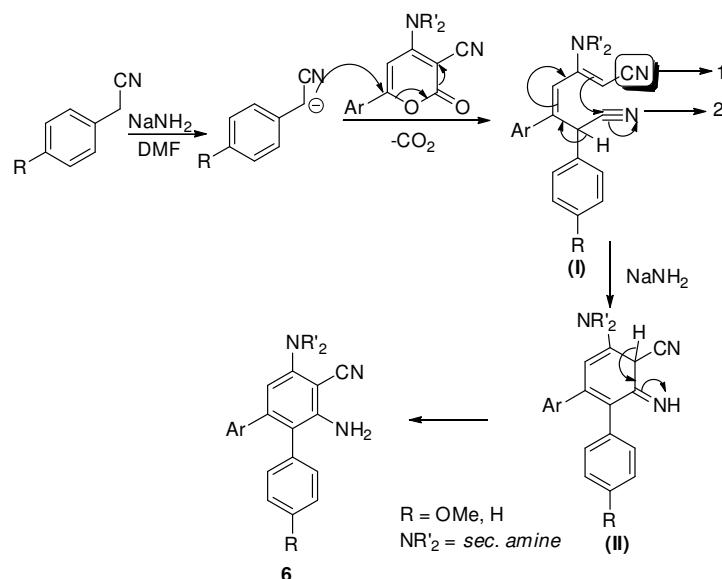


To confirm the role of Microwave assisted heating, we have performed the same reaction on conventional heating bath under nitrogen and aerial atmosphere. It was interesting to observe that under nitrogen atmosphere, we obtained a complex reaction mixture and no formation of **6a** occur probably due to polymerization. While under aerial condition, reaction followed the different path with the formation of 1,5-diphenyl-3-(piperidin-1-yl)cyclopenta-2,4-diene-1,2-dicarbonitrile **7** in 51% yield (Scheme 4). Formation of the product **7** follows the same path as reported earlier.^{19c} From this result, we concluded that Microwave assisted heating is playing an important role for the formation of compound **6**. Probably, since duration of reaction is less in case of Microwave irradiation, So intermediate formed during the reaction immediately undergoes intramolecular cyclization to afford the formation of compound **6**, while in absence of Microwave due to slow reaction rate intermediate interact with molecular oxygen to provide the product **7**.

From structural dissection of 2-pyranone, it is clear that it contains three electrophilic centers *viz.* C2, C4 and C6. Out of these three positions C6 is more electrophilic and soft centre due to presence of nitrile group at C3 and extended conjugation. Mechanistically, we proposed that carbanion generated from benzyl cyanide under basic conditions attack at C6 position of pyran ring followed by decarboxylation via retro Diels-alder approach to afford the intermediate **I** (Scheme 5).

In presence of excess of base again carbanion is generated at benzylic carbon. This carbanion undergoes cyclization involving nitrile group of benzyl cyanide and C3 of pyran ring with

formation of intermediate II. Intermediate II undergoes tautomerization to afford the desired product (Scheme 5).



Scheme 5. Mechanistic approach for the synthesis of functionalized 2-amino-6-aryl-4'-substituted-4-sec-amino-1-[1,1'-biphenyl]-3-carbonitriles **6**

We proposed that moderate yields of desired products were resulted due to formation of sterically hindered intermediate I and II which contain bulkier aromatic ring at adjacent carbon. We also feel that Microwave assisted heating avoids the oxidative decyanation due to lack of oxygen and forced the cyclization for the formation of highly functionalized teraryls. While conventional heating is not sufficient for the cyclization to 1,2-teraryls and also provides oxidative cyclization to afford product **7**. Thus, we proposed that Microwave assisted heating divert the regioselectivity completely.

Molecular Structure Description

The molecular views (ORTEP) for the **6e** with atom numbering scheme are presented in Figure 2. The compound crystallizes in the triclinic system having two molecules in the unit cell. The six membered piperidine ring adopts chair conformation

and the three aromatic rings are essentially planar. The dihedral angle between the central ring and the 4-fluoro phenyl ring is 48.32° and the dihedral angle between the central ring and plain phenyl ring is 65.46°.

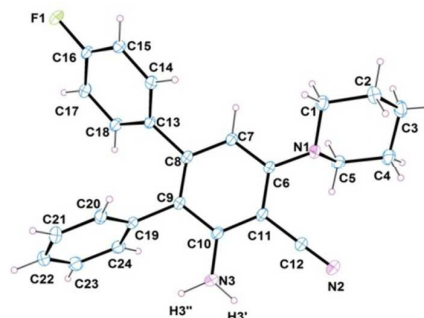


Fig. 2 ORTEP view with atom numbering scheme of **6e** with displacement ellipsoids at the 30% probability level.

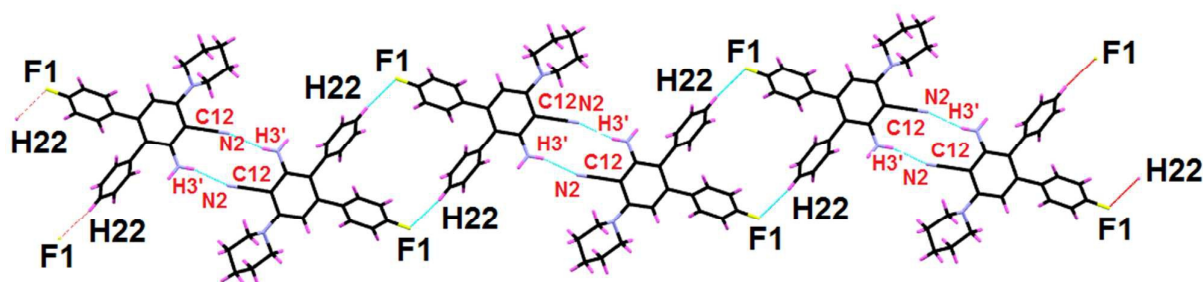


Fig. 3 Supramolecular architecture in **6e** formed by the assistance of weak N-H...N=C and C-H...F halogen bonded interactions

The supramolecular aggregations in **6e** are stabilized by a pair of weak N-H...N=C and C-H...F halogen bonded interactions

(Fig. 3). The cyano group forms a pair of intermolecular interaction with hydrogen atom H3' of the amino group

(2.28(2) Å; 164.6(17)°; symm. op. -x, 2-y, -1-z). Additionally the fluoro group is also involved in weak intermolecular halogen interaction with the aromatic hydrogen of the plain phenyl ring (2.511 Å; 171.09°; symm. op. 1-x, 1-y, -z). On the basis of the interaction distance and angle parameters it can be said that the second interaction is stronger than that of the first one.

DFT and AIM results regarding non-covalent interactions

The crystal structure of **6e** discussed above is good example of the interplay of two different molecular interactions that lead to interesting supramolecular aggregates in the solid state (Fig. 3). It is obvious that N-H...N≡C and C-H...F non-covalent interactions play an important role if the structure is to be rationalized in terms of interactions between the molecular fragments. However, it needs to be investigated to what kind of intermolecular interaction(s) contributes to the binding energy between molecules and dimers in the structure. It is known that the covalent, H-bond, dipole-dipole, and Van der Waals interaction energies are >1700, 70 - 50, 8 - 2, and < 4 kJ/mol, respectively. In order to analyze the various interactions that lead to the crystal structure, interaction energies and electrostatic potentials have been calculated for dimers held by the aforementioned interactions.

The analysis of the interaction energies in the crystal structure of **6e** by means of dimer units at the BSSE-corrected MP2 level of theory yields an interaction energy of -32 kJ/mol in the N-H...N≡C dimer; the interaction energy of the C-H...F dimer is calculated to be -17 kJ/mol. Additionally, the interaction energy for the trimer motif having both N-H...N≡C and C-H...F interactions comes out to be -47 kJ/mol which indicates that there is no cooperatively effect between thesetwo types of interactions. The different intermolecular

interaction energies for both the compounds are in the range between 30-15 kJ/mol, which is well beyond the range of H-bond or dipole-dipole interactions.

To further confirm the presence of these interactions, bond critical points (bcp) were calculated for dimers by using the Atoms in Molecules (AIM) theory.²⁰ The bond critical points observed between the H and N and H and F confirms the

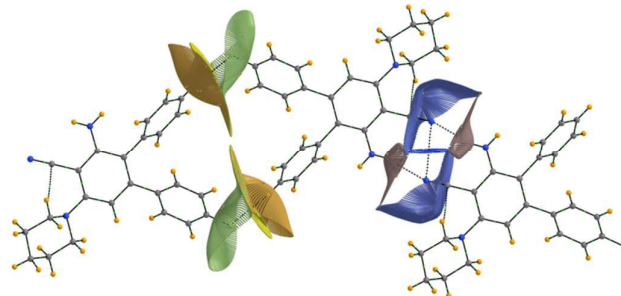


Fig. 4 Molecular graph for trimer of **6e** displaying intermolecular C≡N...H and C-H...F with interatomic surfaces for the atoms of interest (fluorine= green, nitrogen = blue and hydrogen = orange).

presence of N-H...N≡C and C-H...F non-covalent interactions. The interactions have further been corroborated by calculating the interatomic surfaces between the atoms of interest which bisects at the corresponding bond critical points (Fig. 4). The values of electron density (ρ); Laplacian ($\nabla^2 \rho_{\text{bcp}}$); bond ellipticity (ϵ), Hamiltonian form of the Kinetic Energy (K), Potential Energy density (V), Lagrangian form of Kinetic Energy (G) at the bond critical points between pertinent atoms are presented in Table 2.

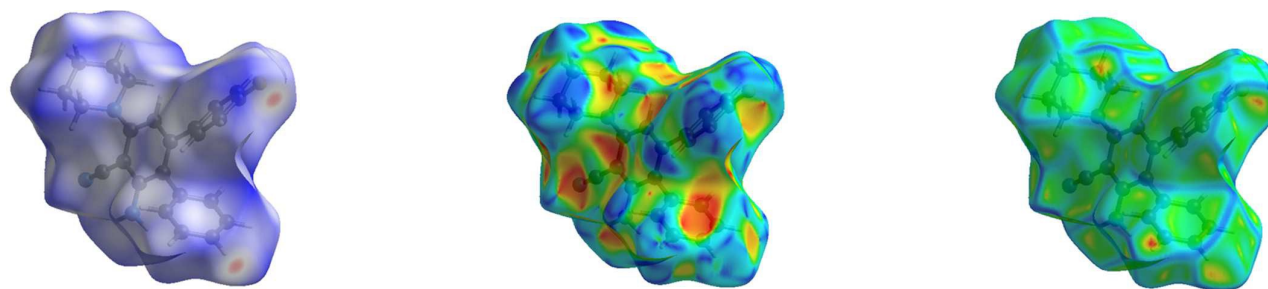


Fig. 5. Hirshfeld surfaces mapped with d_{norm} (left), shape index (middle) and curvedness (right) for **6e**.

From table 2 it is evident that the electron density for all types of interactions at bond critical point (pbcp) are less than +0.10 au which indicates a closed shell hydrogen bonding interactions.²¹ Additionally, the Laplacian of the electron density $\nabla^2 \rho_{\text{bcp}}$ in all the cases are greater than zero which indicates the depletion of electron density in the region of contact between the N-H...N≡C and C-H...F non-covalent interactions. The bond ellipticity (ϵ) measures the extent to which the density is preferentially accumulated in a given plane containing the bond path.²¹ The ϵ values for all the

interactions indicate that these are not cylindrically symmetrical in nature.²¹ The total electron energy density ($H_{\text{b}} = G + V$) associated with these interactions indicates that they are not associated with the significant sharing of electrons and hence confirming the weak non-covalent interaction nature for the two atomic centers. Since for trimer the topological features are remaining unchanged which corroborates the results of MP2 calculations which indicates non-cooperative phenomenon between these interactions.

Method

Organic Chemistry Frontiers

Table 2. Selected topographical features of inter-molecular N-H...N≡C and C-H...F interaction computed at MP2/6-31G** level of theory for dimers and trimer of **6e**.

Interaction	ρ_{bcp}	$\nabla^2\rho_{\text{bcp}}$	(ϵ)	K	V	G
C≡N...H dimer						
C≡N...H	+0.0138	+0.0450	+0.0243	-0.0008	-0.0096	+0.0104
C-H...F dimer						
C-H...F	+0.0070	+0.0284	+0.0093	-0.0011	-0.0049	+0.0060
Trimer held by C≡N...H and C-H...F interactions						
C≡N...H	+0.0138	+0.0450	+0.0243	-0.0008	-0.0096	+0.0104
C-H...F	+0.0070	+0.0284	+0.0093	-0.0011	-0.0049	+0.0060

Hirshfeld Surface Analysis

The Hirshfeld surfaces of the compound **6e** are illustrated in Figure 5, showing surfaces that have been mapped over a d_{norm}

range of -0.5 to 1.5 Å, shape index (-1.0 to 1.0 Å) and curvedness (-4.0 to 0.4 Å). The surfaces are shown as transparent to allow visualization of the aromatic as well as the puckered ring moieties around which they were calculated. The weak interaction information discussed in X-ray crystallography section is summarized effectively in the spots, with the large circular depressions (deep red) visible on the d_{norm} surfaces indicative of hydrogen bonding contacts. The dominant interactions between N-H...NC and C-H...F interactions for the compound can be seen in Hirshfeld surface plots as the bright red shaded area in Figure 5. The small extent of area and light color on the surface indicates weaker and longer contact other than hydrogen bonds.

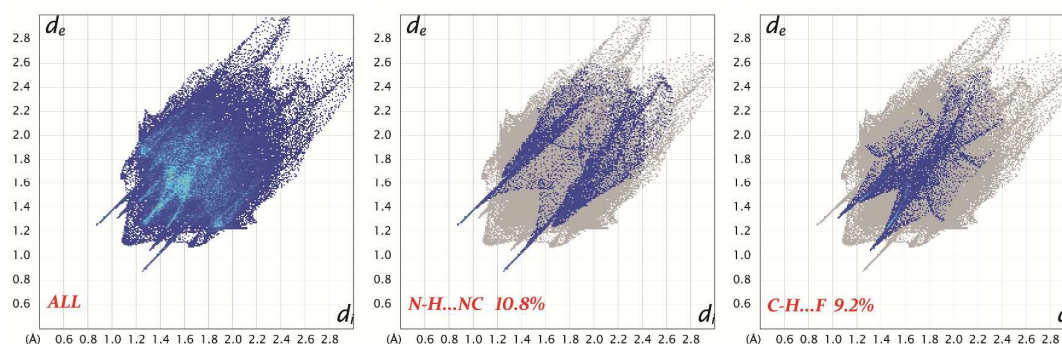


Fig. 6. Fingerprint plots Full (left), resolved into N-H...NC/ CN...H-N (middle) and C-H...F...H-C (right) the title compound showing percentages of contact contributed to the total Hirshfeld surface area of the molecules

The fingerprint plots for **6e** are presented in Fig. 6. The N-H...NC and C-H...F intermolecular interactions appear as two distinct spikes of almost equal lengths in the 2D fingerprint plots in the region $2.03 \text{ \AA} < (d_e + d_i) < 2.47 \text{ \AA}$ as light sky-blue pattern in full fingerprint 2D plots. Complementary regions are visible in the fingerprint plots where one molecule acts as a donor ($d_e > d_i$) and the other as an acceptor ($d_e < d_i$). The fingerprint plots can be decomposed to highlight particular atom pair close contacts. This decomposition enables separation of contributions from different interaction types, which overlap in the full fingerprint. The proportions of N-H...NC/ CN...H-N interactions comprising 10.8% of the total Hirshfeld surface, while the proportion of C-H...F...H-C interactions comprises 9.2% of the total Hirshfeld surface for each molecule of **6e**.

Conclusions

In conclusion, we have developed a simple, efficient and regio-divergent Microwave assisted route for the synthesis of 2-amino-6-aryl-4-sec.amino-biphenyl-3-carbonitriles. We have also studied and compared the influence of Microwave assisted heating with conventional heating on the reactions and isolated two different product. In the presented approach

use of expensive metal catalyst, expensive chemicals and harsh reaction condition was avoided. Hence, it can be concluded that the present investigation can provide economical synthetic pathway for the synthesis of synthesis of 2-amino-6-aryl-4-sec.amino-biphenyl-3-carbonitriles. We have also tried to study the effect of functional group present in pyran ring on the yield of reaction. Weak N-H...N≡C and C-H...F halogen bonded interactions in **6e** led to the formation of one dimensional supramolecular architecture which was addressed using *ab initio*, AIM calculations blended with Hirshfeld surface analysis.

Experimental Section

General remarks Commercial available reagents were used without further purification. IR spectra were recorded on a Perkin-Elmer AX-1 spectrometer in wave number (cm^{-1}). The ^1H NMR (400MHz) and ^{13}C NMR (100MHz) recorded in CDCl_3 solution with reference of CDCl_3 and coupling constant J was reported in Hz. Internal signal patterns was reported as a m, multiplet; dd double doublet; t, triplet; d, doublet; s, singlet. Mass spectra analysis was performed by (ESI) MS spectrometer.

General Procedure synthesis for 2-amino-6-aryl-4'-substituted-4-sec.amino-1-[1,1'-biphenyl]-3-carbonitriles: A solution of 6-aryl-2-oxo-4-sec.amino-2H-pyran-3-carbonitriles **4** (0.5 mmol) and benzylcyanide **5** (0.5 mmol) in DMF (2.0 mL) was prepared in microwave vial followed by addition of NaNH₂ (0.75mmol). Then reaction mixture was flushed with nitrogen and placed in microwave reactor. Reaction was performed under microwave irradiation at 100 °C using maximum 200 watt power for 20 minutes. After completion, reaction mixture was poured onto crushed ice with constant stirring. Then reaction mixture was neutralized with 10% HCl and obtained precipitate was filtered and dried over Na₂SO₄ and purified by silica gel column chromatography using ethylacetate/hexane (1:9) as an eluent.

3'-amino-5'-piperidin-1-yl-[1,1',2',1'']terphenyl-4'-carbonitrile 6a;

Yield: 70% (0.070 g); 0.72 R_f (20% ethylacetate-hexane), Orange solid; mp: 148-150 °C; IR (KBr): 3387, 2928, 2856, 2207 cm⁻¹; ¹H NMR (400 MHz, CDCl₃): δ 1.47-1.63 (m, 2H, -CH₂-), 1.66-1.80 (m, 4H, -CH₂-), 3.10-3.16 (m, 4H, -CH₂-), 4.33 (s, 2H, -NH₂), 6.30 (s, 1H, ArH), 6.93-6.98 (m, 2H, ArH), 6.99-7.03 (m, 2H, ArH), 7.04-7.09 (m, 3H, ArH), 7.10-7.15 (m, 1H, ArH), 7.16-7.22 (m, 2H, ArH); ¹³C NMR (100 MHz, CDCl₃): δ 24.2, 26.1, 53.2, 89.5, 109.4, 117.7, 119.2, 126.8, 127.2, 127.6, 128.7, 129.2, 130.9, 136.1, 141.1, 146.8, 149.0, 156.2; HRMS (ESI) calculated for C₂₄H₂₃N₃, 354.1965 (MH⁺); found for *m/z* 354.1965.

3'-Amino-4-methyl-5'-piperidin-1-yl-[1,1',2',1'']terphenyl-4'-carbonitrile 6b; Yield: 64% (0.062 g); 0.70 R_f (20% ethylacetate-hexane), Orange solid; mp: 140-142 °C; IR (KBr): 3356, 2934, 2852, 2215 cm⁻¹; ¹H NMR (400 MHz, CDCl₃): δ 1.46-1.57 (m, 2H, -CH₂-), 1.67-1.75 (m, 4H, -CH₂-), 2.17 (s, 3H, -CH₃), 3.11 (t, *J* = 5.5 Hz, 4H, -CH₂-), 4.31 (s, 2H, -NH₂), 6.28 (s, 1H, ArH), 6.80-6.92 (m, 4H, ArH), 6.98-7.04 (m, 2H, ArH), 7.11-7.23 (m, 2H, ArH), 7.23-7.34 (m, 1H, ArH); ¹³C NMR (100 MHz, CDCl₃): δ 21.0, 24.2, 26.1, 53.2, 89.4, 109.5, 117.8, 119.1, 127.2, 128.3, 128.7, 129.0, 130.9, 136.2, 136.5, 138.1, 146.7, 149.8, 156.2; HRMS (ESI) calculated for C₂₅H₂₅N₃, 368.2121 (MH⁺); found for *m/z* 368.2128.

3'-Amino-4-chloro-5'-piperidin-1-yl-[1,1',2',1'']terphenyl-4'-carbonitrile 6c; Yield: 59% (0.056 g); 0.69 R_f (20% ethylacetate-hexane), Orange solid; mp: 176-178 °C; IR (KBr): 3357, 2931, 2853, 2209 cm⁻¹; ¹H NMR (400 MHz, CDCl₃): δ 1.55-1.66 (m, 2H, -CH₂-), 1.74-1.84 (m, 4H, -CH₂-), 3.19 (t, *J* = 5.5 Hz, 4H, -CH₂-), 4.40 (s, 2H, -NH₂), 6.32 (s, 1H, ArH), 6.91-6.98 (m, 2H, ArH), 7.02-7.13 (m, 4H, ArH), 7.19-7.32 (m, 3H, ArH); ¹³C NMR (100 MHz, CDCl₃): δ 24.0, 25.9, 53.2, 89.6, 109.3, 117.5, 119.2, 127.5, 127.8, 128.9, 130.4, 130.8, 132.9, 135.7, 139.4, 145.5, 149.2, 155.6; HRMS (ESI) calculated for C₂₄H₂₂ClN₃, 388.1585 (MH⁺); found for *m/z* 388.1587.

3'-amino-4-chloro-4'-methoxy-5'-piperidin-1-yl-[1,1',2',1'']terphenyl-4'-carbonitrile 6d;

Yield: 58% (0.058 g); 0.60 R_f (30% ethylacetate-hexane), Orange solid; mp: 174-176 °C; IR (KBr): 3381, 2955, 2848, 2207 cm⁻¹; ¹H NMR (400 MHz, CDCl₃): δ 1.75 (br m, 6H, -CH₂-), 3.15 (br m, 4H, -CH₂-), 3.76 (s, 3H, -OMe), 4.88 (s, 2H, -NH₂), 6.25 (s, 1H, ArH), 6.79 (d, *J* = 8.4 Hz, 2H, ArH), 6.94 (d, *J* = 8.4 Hz, 4H,

ArH), 7.09 (d, *J* = 8.4 Hz, 2H, ArH); ¹³C NMR (100 MHz, CDCl₃): δ 26.1, 29.6, 53.2, 55.1, 89.7, 109.0, 114.3, 117.6, 118.7, 127.8, 130.5, 132.0, 132.8, 139.7, 145.6, 149.5, 156.2, 158.7; HRMS (ESI) calculated for C₂₅H₂₄ClN₃O, 418.1681 (MH⁺); found for *m/z* 418.1693.

3'-amino-4-fluoro-5'-piperidin-1-yl-[1,1',2',1'']terphenyl-4'-carbonitrile 6e; Yield: 58% (0.052 g); 0.69 R_f (20% ethylacetate-hexane), Orange solid; mp: 188-190 °C; IR (KBr): 3352, 2920, 2851, 2208 cm⁻¹; ¹H NMR (400 MHz, CDCl₃): δ 1.53-1.66 (m, 2H, -CH₂-), 1.70-1.85 (m, 4H, -CH₂-), 3.18 (t, *J* = 5.4 Hz, 4H, -CH₂-), 4.39 (s, 2H, -NH₂), 6.30 (s, 1H, ArH), 6.78-6.86 (m, 2H, ArH), 6.95-7.02 (m, 2H, ArH), 7.03-7.09 (m, 2H, ArH) 7.19-7.31 (m, 3H, ArH); ¹³C NMR (100 MHz, CDCl₃): δ 24.1, 26.1, 53.1, 89.6, 109.2, 114.5 (d, *J*_{C-F} = 21.1 Hz), 117.6, 119.1, 127.3, 128.8, 130.7 (d, *J*_{C-F} = 7.7 Hz), 130.9, 135.9, 137.0, 145.7, 149.1, 156.2, 161.7 (d, *J*_{C-F} = 247.3 Hz); HRMS (ESI) calculated for C₂₄H₂₂FN₃, 372.1871 (MH⁺); found for *m/z* 372.1870.

2-amino-4-piperidin-1-yl-6-thiophen-2-yl-biphenyl-3-carbonitrile 6f;

Yield: 62% (0.057 g); 0.55 R_f (20% ethylacetate-hexane), Orange solid; mp: 175-177 °C; IR (KBr): 3355, 2938, 2855, 2205 cm⁻¹; ¹H NMR (400 MHz, CDCl₃): δ 1.50-1.66 (m, 2H, CH₂), 1.72-1.86 (m, 4H, CH₂), 3.17 (t, *J* = 5.1 Hz, 4H, CH₂), 4.30 (s, 2H, -NH₂), 6.50 (s, 1H, ArH), 6.62-6.66 (m, 1H, ArH), 6.76-6.81 (dd, *J* = 3.6 Hz, 1H, ArH), 7.10-7.20 (m, 3H, ArH), 7.30-7.42 (m, 3H, ArH); ¹³C NMR (100 MHz, CDCl₃): δ 24.2, 26.1, 53.1, 89.5, 108.9, 117.6, 118.6, 126.3, 126.7, 127.4, 128.0, 129.2, 130.9, 136.1, 138.6, 142.6, 149.3, 156.3; HRMS (ESI) calculated for C₂₂H₂₁N₃S, 360.1529 (MH⁺); found for *m/z* 360.1529.

3'-amino-5'-morpholin-4-yl-[1,1',2',1'']terphenyl-4'-carbonitrile 6g;

Yield: 65% (0.062 g); 0.50 R_f (30% ethylacetate-hexane), Orange solid; mp: 181-183 °C; IR (KBr): 3377, 2916, 2843, 2201 cm⁻¹; ¹H NMR (400 MHz, CDCl₃): δ 3.15 (t, *J* = 4.6 Hz, 4H, CH₂), 3.83 (t, *J* = 4.6 Hz, 4H, CH₂), 4.38 (s, 2H, -NH₂), 6.22 (s, 1H, ArH), 6.83 (d, *J* = 8.4 Hz, 2H, ArH), 6.83 (d, *J* = 6.9 Hz, 2H, ArH), 7.15-7.26 (m, 6H, ArH); ¹³C NMR (100 MHz, CDCl₃): δ 51.9, 66.9, 89.6, 108.7, 117.3, 120.0, 121.4, 127.7, 129.0, 130.7, 130.8, 130.9, 135.3, 139.7, 145.7, 149.4, 154.9; HRMS (ESI) calculated for C₂₃H₂₁N₃O, 356.1757 (MH⁺); found for *m/z* 356.1752.

3'-amino-4-bromo-4'-methoxy-5'-morpholin-4-yl-[1,1',2',1'']terphenyl-4'-carbonitrile 6h;

Yield: 62% (0.074 g); 0.35 R_f (30% ethylacetate-hexane), Orange solid; mp: 183-185 °C; IR (KBr): 3389, 2921, 2852, 2210 cm⁻¹; ¹H NMR (400 MHz, CDCl₃): δ 3.19 (t, *J* = 4.6 Hz, 4H, -CH₂-), 3.76 (s, 3H, -OMe), 3.88 (t, *J* = 4.6 Hz, 4H, -CH₂-), 4.44 (s, 2H, -NH₂), 6.25 (s, 1H, ArH), 6.80 (d, *J* = 8.4 Hz, 2H, ArH), 6.88 (d, *J* = 8.4 Hz, 2H, ArH), 6.94 (d, *J* = 8.4 Hz, 2H, ArH), 7.22-7.29 (m, 2H, ArH); ¹³C NMR (100 MHz, CDCl₃): δ 51.9, 55.1, 66.9, 89.5, 108.7, 114.4, 117.4, 119.8, 121.2, 127.3, 130.7, 130.9, 131.9, 139.8, 145.9, 149.8, 154.7, 158.8; HRMS (ESI) calculated for C₂₄H₂₂BrN₃O₂, 464.0968 (MH⁺); found for *m/z* 464.0975.

3'-amino-4-chloro-5'-morpholin-4-yl-[1,1',2',1'']terphenyl-4'-carbonitrile 6i;

Yield: 64% (0.066 g); 0.34 R_f (30% ethylacetate-hexane), Orange solid; mp: 17 °C; IR (KBr): 3377, 2919, 2848, 2208 cm⁻¹; ¹H NMR (400 MHz, CDCl₃): δ 3.20 (t, *J* = 4.2 Hz, 4H, -CH₂-),

Method

Organic Chemistry Frontiers

3.88 (t, $J = 4.6$ Hz, 4H, $-\text{CH}_2-$), 4.43 (s, 2H, $-\text{NH}_2$), 6.27 (s, 1H, ArH), 6.93 (d, $J = 8.6$ Hz, 2H, ArH), 7.04 (d, $J = 6.9$ Hz, 2H, ArH), 7.09 (d, $J = 8.4$ Hz, 2H, ArH), 7.20-7.31 (m, 3H, ArH); ^{13}C NMR (100 MHz, CDCl_3): δ 51.9, 66.9, 89.6, 108.7, 117.3, 120.0, 127.6, 127.9, 129.0, 130.4, 130.7, 133.0, 135.4, 139.2, 145.7, 149.4, 154.9; HRMS (ESI) calculated for $\text{C}_{23}\text{H}_{20}\text{ClN}_3\text{O}$, 390.1368 (MH^+); found for m/z 390.1377.

3'-amino-4-fluoro-4''-methoxy-5'-morpholin-4-yl-[1,1',2',1'']terphenyl-4'-carbonitrile 6j;

Yield: 64% (0.063 g); 0.36 R_f (30% ethylacetate-hexane), Orange solid; mp: 212-214 °C; IR (KBr): 3377, 2949, 2839, 2206 cm^{-1} ; ^1H NMR (400 MHz, CDCl_3): δ 3.19 (br m, 4H, $-\text{CH}_2-$), 3.75 (s, 3H, $-\text{OMe}$), 3.83-3.92 (m, 4H, $-\text{CH}_2-$), 4.43 (s, 2H, $-\text{NH}_2$), 6.27 (s, 1H, ArH), 6.76-6.90 (m, 4H, ArH), 6.91-7.04 (m, 5H, ArH); ^{13}C NMR (100 MHz, CDCl_3): δ 51.9, 55.1, 67.0, 89.4, 108.8, 114.4, 114.7 (d, $J = 21.0$ Hz), 117.5, 120.0, 127.4, 130.7 (d, $J = 7.7$ Hz), 131.9, 136.9, 146.1, 149.6, 154.7, 159.7 (d, $J = 178.3$ Hz); HRMS (ESI) calculated for $\text{C}_{24}\text{H}_{22}\text{FN}_3\text{O}_2$, 404.1769 (MH^+); found for m/z 404.1769.

1,5-diphenyl-3-(piperidine-1-yl)cyclopenta-2,4-diene-1,2-dicarbonitrile 7;

A mixture of 2-oxo-6-phenyl-4-(piperidin-1-yl)-2H-pyran-3-carbonitriles (0.5 mmol) and benzylocyanide 5 (0.5 mmol) and powdered NaNH_2 (1.0 mmol) in DMF (4.0 mL) was stirred at 100 °C temperature for 3h. Completion of reaction was monitored by TLC. After completion, reaction mixture was poured onto ice-water with constant stirring followed by neutralization with 10% HCl. The precipitate obtained was filtered, washed with cold water, dried and purified through column chromatography using 15 % ethyl acetate in hexane as an eluent. Yield: 51% (0.089 g), 0.2 R_f (15% ethylacetate-hexane): Green solid; mp: 118-120 °C; ^1H NMR (400 MHz, CDCl_3): δ 1.69-176 (br s, 6H, $-\text{CH}_2-$), 3.64-3.71 (br s, 4H $-\text{CH}_2-$), 7.06 (s, 1H, $-\text{CH}-$), 7.23-7.40 (m, 8H, ArH), 7.41-7.47 (m, 2H, ArH); ^{13}C NMR (100 MHz, CDCl_3): δ 23.8, 25.7, 49.7, 57.2, 81.4, 118.0, 118.4, 124.0, 125.5, 126.8, 128.5, 128.8, 129.3, 129.7, 130.4, 134.0, 151.7, 158.4; HRMS (ESI) calculated for $\text{C}_{24}\text{H}_{22}\text{N}_3$, 352.1808 (MH^+); found for m/z , 352.1817.

X-ray Crystallography

Intensity data for **6e** was collected at 298(2) K on an Agilent Xcalibur diffractometer using graphite monochromated Mo-K α radiation $\lambda = 0.71073$ Å. Unit cell determination, data collection and data reduction were performed with CrysAlisPro.²² The structure was solved by direct methods (SIR97)²³ and refined by a full-matrix least-squares procedure based on F^2 .²⁴ All non-hydrogen atoms were refined anisotropically; hydrogen atoms were located at calculated positions and refined using a riding model. All hetero hydrogen atoms have been located in the difference Fourier map and were refined with bond lengths restraints.

Crystal Data **6e**: CCDC 1439536 $\text{C}_{24}\text{H}_{22}\text{FN}_3$, $M = 251.30$, Triclinic, P-1, $a = 10.0016(5)$ Å, $b = 10.9336(5)$ Å, $c = 11.1245(6)$ Å, $\alpha = 105.508(4)^\circ$, $\beta = 106.640(4)^\circ$, $\gamma = 110.161(4)^\circ$, $V = 999.42(9)$ Å³, $Z=2$, $D_{\text{calc}}=1.234$ mg m⁻³, $F(000) = 392$, crystal size $0.220 \times 0.200 \times 0.190$ mm, reflections collected 16065, independent reflections 4826 [$R(\text{int}) = 0.0226$], Final indices [$I > 2\sigma(I)$] $R1 = 0.0539$, $wR2 = 0.1288$, R indices (all data) $R1 =$

0.0728, $wR2 = 0.1419$, $\text{gof} = 0.930$, Largest difference peak and hole 0.213 and -0.153 e Å⁻³.

Computational details

Molecular geometries were optimized at the level of density functional theory (DFT) using the B3LYP functional.²⁵ The split valence basis sets, 6-31G** were used at all the atom centers. The intermolecular interaction energies have been estimated at the MP2 level of theory.²⁶ For the interaction energy calculations, the interaction distances have been fixed for the dimer while all other degrees of freedom were relaxed in the geometry optimization. The stabilization energies (ΔE_{dimer} and ΔE_{trimer}) for dimeric and trimeric motifs involving the 2 and 3 molecules, respectively were calculated using the formula $\Delta E_{\text{dimer}} = E_{\text{dimer}} - (2 \times E_{\text{monomer}})$ where E_{monomer} , E_{dimer} are the energies of the monomer and dimer motifs. E_{monomer} was calculated by optimizing a single molecule at the same level of theory. The intermolecular interaction strengths are significantly weaker than either ionic or covalent bonding, therefore it was essential to do basis set superposition error (BSSE) corrections. The BSSE corrections in the interaction energies were done using Boys-Bernardi scheme. In this paper all the interaction energies have been reported after BSSE correction.²⁷ All computational experiments have been performed using the Gaussian 09 programme.²⁸

Hirshfeld Surface Analysis

Molecular Hirshfeld surfaces²⁹ in the crystal structure were constructed on the basis of the electron distribution calculated as the sum of spherical atom electron densities.^{30,31} For a given crystal structure and a set of spherical atomic densities, the Hirshfeld surface is unique.³² The normalized contact distance (d_{norm}) based on both d_e and d_i (where d_e is distance from a point on the surface to the nearest nucleus outside the surface and d_i is distance from a point on the surface to the nearest nucleus inside the surface) and the vdW radii of the atom, as given by eq 1 enables identification of the regions of particular importance to intermolecular interactions.²⁹ The combination of d_e and d_i in the form of two-dimensional (2D) fingerprint plot^{33,34} provides a summary of intermolecular contacts in the crystal.²⁹ The Hirshfeld surfaces mapped with d_{norm} and 2D fingerprint plots were generated using the Crystal-Explorer 3.1.³⁵ Graphical plots of the molecular Hirshfeld surfaces mapped with d_{norm} used a red-white-blue colour scheme, where red highlight shorter contacts, white represents the contact around vdW separation, and blue is for longer contact.³⁶

$$d_{\text{norm}} = \frac{d_i - r_i^{\text{vdW}}}{r_i^{\text{vdW}}} + \frac{d_e - r_e^{\text{vdW}}}{r_e^{\text{vdW}}} \quad (1)$$

Acknowledgements

RP thank Department of Science and Technology (DST, New Delhi) [Project No. SB/FT/CS-049/2012 and Purse grant], Council of Scientific and Industrial Research (CSIR, New Delhi) [Project No. 02(0080)/12/EMR-II], and University of Delhi,

Delhi [R & D Grant] for financial support. SS and RS thank Council of Scientific and Industrial Research (CSIR, New Delhi) and S thanks UGC for research fellowship. Authors thank USIC, Delhi University for providing instrumentation facility. RP thank Dr. Vishnu Ji Ram for his valuable suggestions.

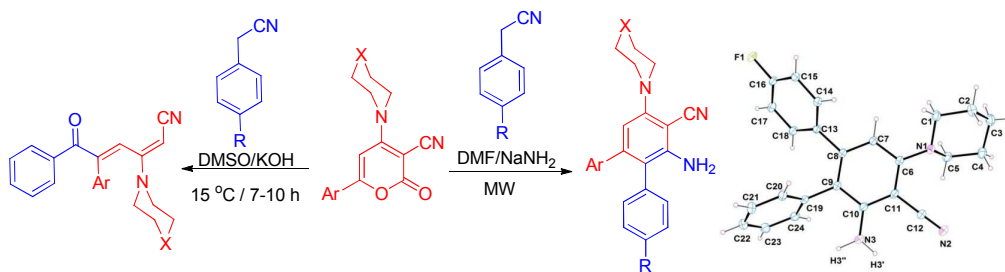
References

- (a) C. S. Hampton, M. Harmata *Org. Lett.* 2014, **16**, 1256–1259; (b) D. Comegna, M. DellaGreca, M. R. Iesce, L. Previtera, A. Zarrella and S. Zuppolina *Org. Biomol. Chem.*, 2012, **10**, 1219–1224; (c) L. C. Miller, R. Sarpong *Chem. Soc. Rev.*, 2011, **40**, 4550–4562; (d) P. Yadav, S. Singh, S. N. Sahu, F. Hussain, R. Pratap *Org. Biomol. Chem.*, 2014, **12**, 2228–2234.
- (a) J. Hassan, M. Sévignon, C. Gozzi, E. Schulz, M. Lemaire, *Chem. Rev.* 2002, **102**, 1359; (b) D. J. Schneider, D. A. Landis, P. A. Fleitz, C. J. Seliskar, J. M. Kaufman, R. N. Steppel, *Laser Chem.* 1991, **11**, 49.
- G. W. Gary, P. A. Winsor, *Liquid Crystal and Plastic Crystal*, John Wiley and Sons. New York, 1974, Vol.1.
- (a) K. N. Baker, A. V. Fratini, T. Resch, H. C. Knachel, W. W. Adams, E. P. Soggi, B. L. Farmer, *Polymer* 1993, **34**, 1571. (b) W. Kern, W. Heitz, H. O. Wirth, *Makromol. Chem.* 1961, **42**, 177.
- B. Basu, P. Das, M. Mosharef, H. Bhuiyan, S. Jha, *Tetrahedron Lett.* 2003, **44**, 3817.
- (a) J. M. Trujillo, R. E. Jorge, E. Navarro, J. Boada, *Phytochemistry* 1990, **29**, 2991. (b) K. Tsuji, K. Nakamura, T. Ogino, N. Konishi, T. Tojo, T. Ochi, N. Seki, M. Matsuo, *Chem. Pharm. Bull.* 1998, **46**, 279.
- (a) K. Weissmermel, H. J. Arpe, *Industrial Organic Chemistry*, WileyVCH, Weinheim, Germany, 1997; (b) Lawrence, S. A. *Amines: Synthesis, Properties, and Application*; Cambridge University Press: Cambridge, 2004.
- (a) J. A. J. Hore, C. C. C. Johansson, M. Gulias, E. M. Beck and M. J. Gaunt, *J. Am. Chem. Soc.* 2008, **130**, 16184. (b) Q. Jiang, D. Duan-Mu, W. Zhong, H. Chen and H. Yan, *Chem. Eur. J.* 2013, **19**, 1903.
- S. W. Youn, J. H. Bihn, *Tetrahedron Lett.* 2009, **50**, 4598.
- M. Rakotomalala, M. Ciesielski, T. Zevaco and M. Doering, *Phosphorus, Sulfur and Silicon* 2011, **186**, 989.
- J. Albert, J. Granell, J. Zafrilla, M. F. Bardia, X. Solans, *J. Organomet. Chem.* 2005, **690**, 422.
- Q. Shen, and J. F. Hartwig, *J. Am. Chem. Soc.* 2006, **128**, 10028.
- R. V. Jagadeesh, G. Wienhofer, F. A. Westerhaus, A. E. Surkus, H. Junge and M. Beller, *Chem. Eur. J.* 2011, **17**, 14375.
- T. Pirali, F. Zhang, A. H. Miller, J. L. Head, D. Mcausland and M. F. Greaney, *Angew. Chem.* 2012, **51**, 1006.
- M. Baghbanzadeh, C. Pilger and C. O. Kappe, *J. Org. Chem.* 2011, **76**, 1507.
- Z. Z. Zhou, F. S. Liu, D. S. Shen, C. Tan, L. Y. Luo, *Inorganic Chemistry Communications* 2011, **14**, 659.
- S. Singh, P. Yadav, S. N. Sahu, A. Sharone, B. Kumar, V. J. Ram, R. Pratap, *Synlett* 2014, **25**, 2599.
- S. Singh, R. Panwar, I. Althagafi, V. Sharma, S. Chaudhary, R. Pratap, *Tetrahedron Lett.* 2015, **56**, 5203.
- Y. Tominaga, A. Ushiroguchi, Y. Matsuda, *J. Heterocycl. Chem.* 1987, **24**, 1557. (b) R. Pratap, B. Kumar, V. Ram, *Tetrahedron* 2006, **34**, 8158. (c) S. Singh, R. Panwar, P. Yadav, I. Althagafi, S. N. Sahu, R. Pratap, *RSC Adv.*, 2015, **5**, 18335–18341.
- R. F. W. Bader, *Atoms in Molecules: A Quantum Theory*; Oxford University Press: New York, 1990.
- C. F. Matta and R. J. Boyd, *The Quantum Theory of Atoms in Molecules: From Solid State to DNA and Drug Design*; Wiley VCH, VerlagGmbH & Co. KGaA: Germany, 2007.
- (a) Z. Otwinowski and W. Minor, "Processing of X-ray Diffraction Data Collected in Oscillation Mode", *Methods in Enzymology, Macromolecular Crystallography, part A.* 1997, **276**, 307. (b) C. W. Carter, Jr and R. M. Sweet, Eds. Academic Press 1997.
- A. Altomare, M. C. Burla, M. Camalli, G. L. Casciarano, C. Giacovazzo, A. Guagliardi, A. G. G. Moliterni, G. Polidori and R. Spagna, *J. Appl. Crystallogr.* 1999, **32**, 115.
- G. M. Sheldrick, *Acta Cryst. A.* 2008, **A64**, 112.
- (a) A. D. Becke, *J. Chem. Phys.*, 1993, **98**, 5648; (b) C. T. Lee, W. T. Yang and R. G. Parr, *Phys. Rev. B: Condens. Matter Mater. Phys.*, 1998, **37**, 1133.
- M. Head-Gordon, J. A. Pople and M. J. Frisch, *Chem. Phys. Lett.*, 1988, **153**, 503–506.
- S. F. Boys and F. Bernardi, *Mol. Phys.*, 1970, **19**, 553.
- M. J. Frisch, G. W. Trucks, H. B. Schlegel, G. E. Scuseria, M. A. Robb, J. R. Cheeseman, J. A. Montgomery, T. Vreven Jr., K. N. Kudin, J. C. Burant, J. M. Millam, S. S. Iyengar, J. Tomasi, V. Barone, B. Mennucci, M. Cossi, G. Scalmani, N. Rega, G. A. Petersson, H. Nakatsuji, M. Hada, M. Ehara, K. Toyota, R. Fukuda, J. Hasegawa, M. Ishida, T. Nakajima, Y. Honda, O. Kitao, H. Nakai, M.; Klene, X. Li, J. E. Knox, H. P. Hratchian, J. B. Cross, V. Bakken, C. Adamo, J. Jaramillo, R. Gomperts, R. E. Stratmann, O. Yazyev, A. J. Austin, R. Cammi, C. Pomelli, J. W. Ochterski, P. Y. Ayala, K. Morokuma, G. A. Voth, P. Salvador, J. J. Dannenberg, V. G. Zakrzewski, S. Dapprich, A. D. Daniels, M. C. Strain, O. Farkas, D. K. Malick, A. D. Rabuck, K. Raghavachari, J. B. Foresman, J. V. Ortiz, Q. Cui, A. G. Baboul, S. Clifford, J. Cioslowski, B. B. Stefanov, G. Liu, A. Liashenko, P. Piskorz, I. Komaromi, R. L. Martin, D. J. Fox, T. Keith, M. A. Al-Laham, C. Y. Peng, A. Nanayakkara, M. Challacombe, P. M. W. Gill, B. Johnson, W. Chen, W. M. Wong, C. Gonzalez and J. A. Pople, Gaussian, Inc., Wallingford CT, 2004.
- M. A. Spackman and J. J. McKinnon, *Cryst. Eng. Comm.*, 2002, **4**, 378–392.
- M. A. Spackman and P. G. Byrom, *Chem. Phys. Lett.*, 1997, **267**, 309.
- J. J. McKinnon, A. S. Mitchell, and M. A. Spackman, *Chem. Eur. J.*, 1998, **4**, 2136–2141.
- J. J. McKinnon, M. A. Spackman and A. S. Mitchell, *Acta Crystallogr. Sec. B*, 2004, **60**, 627–668.
- A. L. Rohl, M. Moret, W. Kaminsky, K. Claborn, J. J. McKinnon and B. Kahr, *Cryst. Growth Des.* 2008, **8**, 4517–4525.
- A. Parkin, G. Barr, W. Dong, C. J. Gilmore, D. Jayatilaka, J. J. McKinnon, M. A. Spackman and C. C. Wilson, *CrystEngComm*, 2007, **9**, 648–652.
- S. K. Wolff, D. J. Greenwood, J. J. McKinnon, D. Jayatilaka and M. A. Spackman, *Crystal Explorer 3.1*; University of Western Australia: Perth, Australia, 2012.
- J. J. Koenderink and A. J. van Doorn, *Image Vision Comput.* 1992, **10**, 557–564.

Graphical Abstract

Microwave directed metal-free regiodivergent synthesis of 1,2-teraryls and study of supramolecular interactions

Surjeet Singh, Shally, Ranjay Shaw, Reena Yadav, Abhinav Kumar and Ramendra Pratap*



Microwave mediated regiodivergent synthesis of highly functionalized 1,2-teraryls has been reported.